



ELSEVIER

Surface Science xxx (2002) xxx–xxx

SURFACE SCIENCE

www.elsevier.com/locate/susc

Corrosion of epitaxial Fe(001) films studied with CEMS and AFM

I. Flis-Kabulska^a, B. Handke^{b,c}, N. Spiridis^b, J. Haber^b, J. Korecki^{b,c,*}

^a Institute of Physical Chemistry, Polish Academy of Sciences, Warszawa, Poland

^b Institute of Catalysis and Surface Chemistry, Polish Academy of Sciences, Kraków, Poland

^c Department of Solid State Physics, Faculty of Physics and Nuclear Techniques, University of Mining and Metallurgy (AGH), al. Mickiewicza 30, 30-059 Kraków, Poland

Abstract

Epitaxial Fe(001) films of a high crystalline and surface quality, as checked in situ with AES, low energy electron diffraction and STM, were grown on MgO(001). Such films show an exceptional corrosion resistance remaining metallic for years at the ambient atmosphere, except of 5–10 nm, as found using the conversion electron Mössbauer spectroscopy (CEMS). For more systematic corrosion studies, 50 nm iron films were prepared of the ⁵⁷Fe isotope. As-prepared Fe films, exposed to the atmosphere did not show clear morphological and compositional changes, which could be associated with the oxide formation, as checked with contact AFM in air and with CEMS. After exposure of the film to HNO₃ or HCl vapors corrosion was observed with AFM. It resulted in two different types of surface modifications. The first one was seen as a homogenous granular layer with the height amplitude of about 15 nm. Corrosion-induced changes of the second type have a localized character resulting in micrometer sized porous protrusions. The corrosion products were identified as γ-FeOOH. Controlled oxidation of surface iron layer to epitaxial Fe₃O₄ passivated the film. © 2002 Published by Elsevier Science B.V.

Keywords: Atomic force microscopy; Scanning tunneling microscopy; Mössbauer spectroscopy; Low energy electron diffraction (LEED); Corrosion; Oxidation; Iron; Epitaxial thin film

1. Introduction

Room temperature atmospheric corrosion of iron and its alloys is probably one of the most common processes touching all of us. Fe exposed to the atmosphere is subjected to different reactions that are governed by the structure and composition of a surface layer and atmospheric

pollutants. Real processes have a complex character and are difficult to be recognized as elementary reactions like passivation, oxidation or corrosion. Whereas wet corrosion under electrochemical conditions has been intensively studied and fairly well understood, less is known about atmospheric corrosion and especially its initial stages. STM and AFM which is used extensively in studies of the surface structure, give new insight in understanding of dissolution and passivation of metals and alloys proceeding during corrosion processes [1–4], including oxidation and passivation of iron, especially in solutions [5–9].

* Corresponding author. Tel.: +48-12-617-2911; fax: +48-12-634-1247.

E-mail address: korecki@uci.agh.edu.pl (J. Korecki).

43 Numerous factors determine corrosion processes. Beside of the individual features of the environment (temperature, humidity, pH), structure of the sample plays a crucial role [3]. A prerequisite for understanding the course of the process is the use of well defined surfaces, which are offered by single crystals. It is due to strong sensitivity of chemical reactions to the coordination, local composition, impurities and defects. In the previous paper [10], corrosion of polycrystalline Fe films in acid vapors was studied using AFM, whereas presently, we extend these studies to corrosion in epitaxial Fe(001) films. The sensitivity of the applied experimental methods—conversion electron Mössbauer spectroscopy (CEMS) and AFM—allowed to follow in nanoscale local changes in composition and morphology of the film surface exposed to air, HNO₃ and HCl atmosphere.

62 The reaction of HNO₃ with the as-prepared films was compared with that occurring on a film, which was oxidized epitaxially to Fe₃O₄.

65 2. Experimental

66 Fe(001) films were grown by molecular epitaxy in a multichamber UHV system described in details elsewhere [11]. To enable further studies with Mössbauer spectroscopy, isotopically pure iron, ⁵⁷Fe and ⁵⁶Fe was used. Iron was evaporated from thermal sources on polished MgO(001) substrates (10 × 10 × 1 mm³) at elevated temperature that was optimized for a flat growth [12]. The film thickness (typically a few tens of nm) was controlled by a quartz balance. The film composition and structure was checked in situ by the Auger electron spectroscopy and low energy electron diffraction (LEED). For in situ Mössbauer measurements samples were transferred into a CEMS UHV chamber. Compared to standard surface sensitive characterization methods, CEMS has the advantage of probing deeper layers (down to 100 nm) with a monolayer resolution [13]. In the course of an UHV experiment, samples could be exposed to a controlled oxygen atmosphere (up to 10⁻⁴ Pa). Freshly prepared samples were taken out from the UHV system through a load-lock, which

88 allowed division of the sample into pieces, usually 89 four. Then the samples were placed in containers 90 under pure N₂ and stored for further studies. Ex 91 situ experiments comprise exposure of the samples 92 to a controlled acidic atmosphere, AFM mea- 93 surements in ambient atmosphere and Mössbauer 94 spectroscopy.

95 AFM topography was examined in a contact 96 mode with Si₃N₄ cantilevers using TopoMetrix 97 Discoverer TMX 2000 system. In another UHV 98 system [14] Fe(001) films obtained under similar 99 conditions as described above, were characterized 100 with STM (Aris 1100, Burleigh, with nanoscope 101 control) at different stages of the thermal and 102 chemical treatment.

3. Samples

104 On MgO(001) Fe grows with epitaxial relations: 105 Fe(001)//MgO(001) and Fe[110]// 106 MgO[100], i.e. by 45° rotation of the (001) sur- 107 face unit cell. A flat growth is reported for Fe on 108 MgO at elevated temperatures [12], but to prevent 109 an island growth, nucleation should proceed at 110 low temperature (e.g. 300 K) and then temperature 111 can be risen gradually up to 620 K at the final 112 thickness. Fig. 1 documents structure of a 50 nm 113 film obtained according to the above receipt. The 114 LEED pattern (not shown) reveals a low back- 115 ground and sharp spots corresponding to mono- 116 atomic terraces seen in the STM image (Fig. 1(a)).

117 Epitaxial Fe(001) films present an exceptional 118 resistance to atmospheric corrosion. Our long- 119 term observation indicates that only after months 120 long storage in laboratory environment, the sam- 121 ples show traces of oxidation. Fig. 1(b) and (c) 122 exemplify the influence of the atmosphere by 123 comparison of CEMS spectra of 50 nm ⁵⁷Fe(001) 124 films taken after one week and one year storage in 125 laboratory air. The spectra are dominated by a six- 126 line pattern of metallic iron. Any oxide phases can 127 be easily detected by contribution in the central 128 part of the spectra for paramagnetic oxides or 129 hydroxides (FeO, γ-FeOOH) or high splitting 130 components for magnetite, hematite, maghemite 131 or goethite. The magnetic phases in a highly dis- 132 persed state often give rise to “nonmagnetic”

103

104

105

106

107

108

109

110

111

112

113

114

115

116

117

118

119

120

121

122

123

124

125

126

127

128

129

130

131

132

133

134

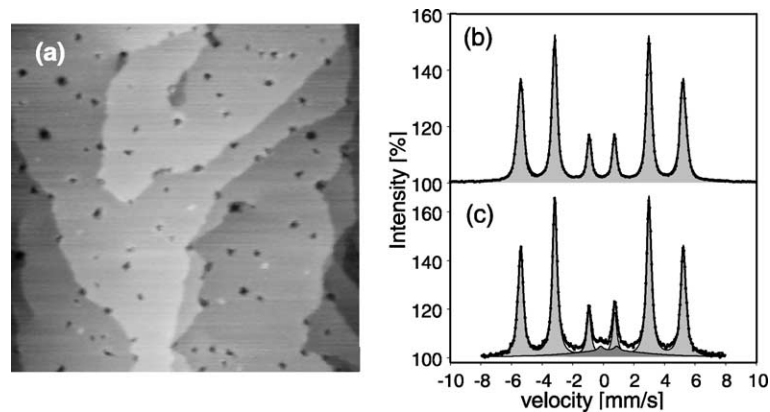


Fig. 1. 50 nm epitaxial Fe(001) film on MgO(001) as characterized by STM and CEMS: (a) $100 \times 100 \text{ nm}^2$ topographic STM image, (b) and (c) CEMS spectra one week after preparation and one year after preparation, respectively.

133 spectra due to superparamagnetism. In the CEMS
 134 detection limit ($\sim 1\%$ of the total film thickness) an
 135 oxide layer after one week storage is certainly
 136 thinner than 0.5 nm, whereas after one year at
 137 variable conditions of humidity and temperature,
 138 the layer of unidentified oxides is 6 ± 1 nm thick.

139 4. Results and discussion

140 To simulate a passive layer formed on Fe(001)
 141 surfaces [15], a Fe(001) film was subjected to ox-
 142 idation at 10^{-4} Pa in UHV chamber by annealing
 143 for 15 min at 550 K. To enhance the surface sensi-
 144 tivity, the sample was engineered by placing a 5

nm ^{57}Fe probe layer on top of a 20 nm ^{56}Fe film. 145
 The oxidation resulted in the formation of a new 146
 epitaxial phase observed in a LEED pattern (Fig. 147
 2(a)). The pattern symmetry indicates that the 148
 layer could be magnetite. STM image showed 149
 distinct changes of the film topography (Fig. 2(b)
 and (c)). Small irregular grains transformed after 150
 annealing to monoatomic terraces with atomically 151
 resolved structures characteristic for magnetite 152
 [16], as shown in the inset on Fig. 2(b). Unam- 153
 biguous identification of the layer formed is given 154
 by a CEMS measurement shown in Fig. 2(d). The 155
 spectrum could be fitted with four components. 156
 The components (A) and (B) come from magnetite 157
 representing Fe ions in tetrahedral and octahedral 158
 159

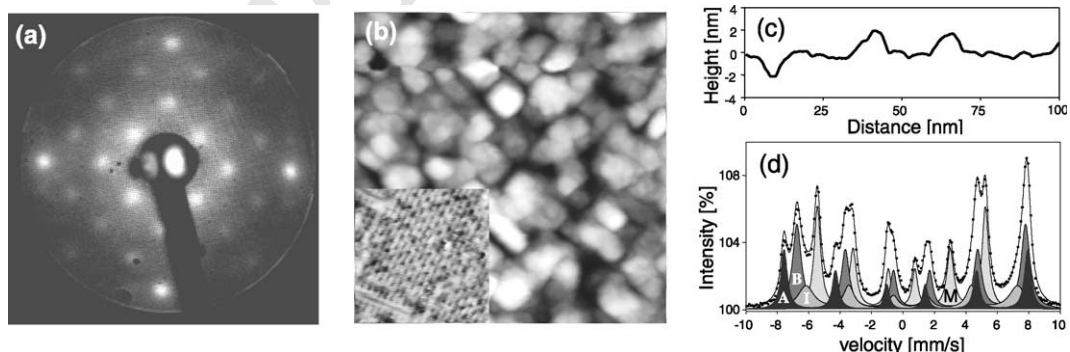


Fig. 2. Oxidized 20 nm $^{56}\text{Fe}/5 \text{ nm } ^{57}\text{Fe}$ epitaxial film on MgO(001) as characterized by LEED, STM and CEMS: (a) LEED pattern at 94 eV, (b), (c) $100 \times 100 \text{ nm}^2$ topographic STM image with a section along the marked line and (d) in situ CEMS spectrum. Inset on (b) shows the $12.5 \times 12.5 \text{ nm}^2$ atomically resolved scan of the film annealed at 750 K.

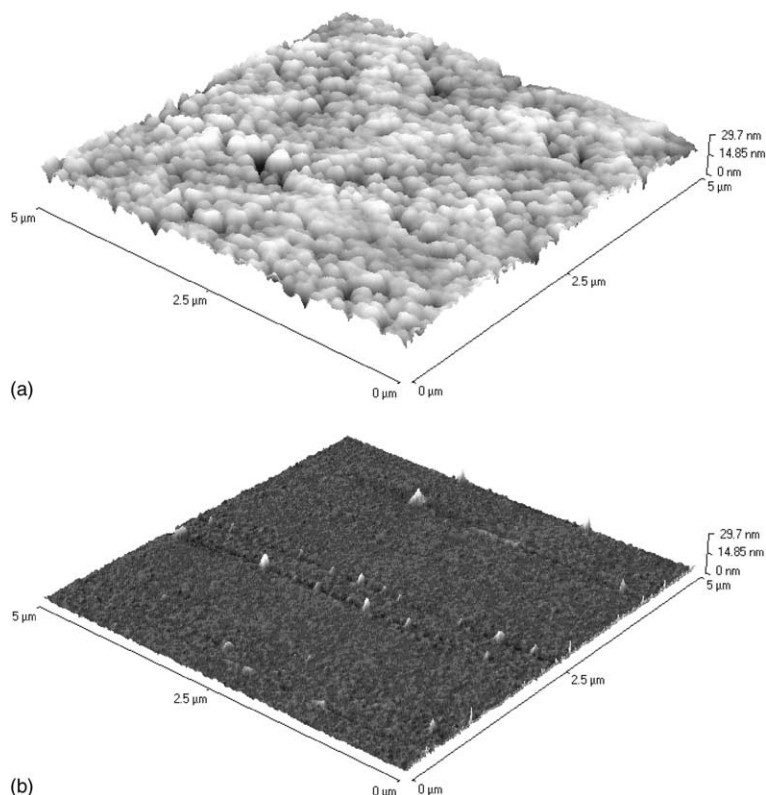


Fig. 3. AFM image of an epitaxial Fe(001) film on MgO(001): (a) after 25 h exposure to 1 M HNO₃ vapors and three weeks storing in air and (b) shortly after preparation.

160 sites, respectively. Component (M) is due to metallic iron. Apparently, the oxidation affected only
161 a part of the top ⁵⁷Fe layer. Component (I) comes probably from an interfacial layer present between
162 Fe₃O₄ and metallic iron. Neglecting differences in recoilless fractions, the thickness of the oxide layer
163 can be estimated by comparing the relative intensity of the spectral components, which yields that
164 the magnetite layer formed on the epitaxial Fe(001) film is 3 nm thick. In the following text
165 this sample will be referred as Fe/Fe₃O₄.

171 To intensify the corrosion process, the samples
172 were exposed for 1 min to 25 h to the atmosphere
173 in equilibrium with vapors of 1 M HNO₃ or 1 M
174 HCl at room temperature. After exposure to cor-
175 roding agents samples were stored in a desiccator.
176 In the saturated atmosphere, an electrolyte is ad-
177 sorbed on the film surface (presumably in form of
178 separated droplets) as a result of the vapor con-

179 densation. In such an experiment, contrary to the
180 processes conducted in a bulk solution where
181 corrosion products partly dissolve, initial stages of
182 localized corrosion could be observed.

183 Corrosion resulted in two different types of
184 surface modifications as observed with AFM. The
185 first one, presented in Fig. 3(a) for a selected 5 × 5
186 μm² area, is seen after a long time exposure (25 h,
187 followed by storing for three weeks in air) as a
188 continuous layer of granules with the height ampli-
189 tude of about 15 nm. For comparison, the AFM
190 topography of the Fe(001) surface before chemi-
191 cal treatment is shown in Fig. 3(b). The surface
192 observed at the initial stage corresponds to the in
193 situ STM image (Fig. 1(a)). Few structures (na-
194 nometer sized) appearing on the atomically flat
195 iron film are probably impurities adsorbed during
196 the sample handling.

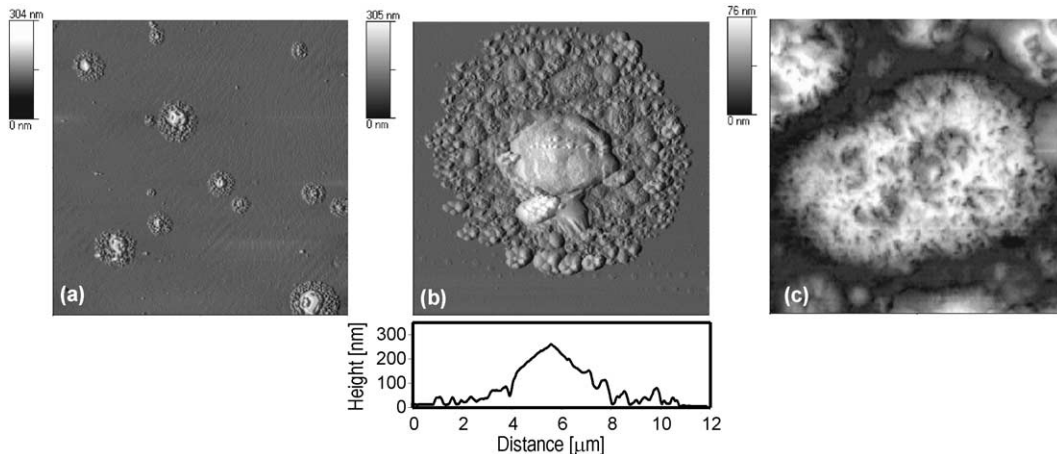


Fig. 4. AFM image of an epitaxial Fe(001) film on MgO(001) after 1 min exposure to 1 M HNO₃ vapors and a subsequent 24 h storing in air: (a) large area 70 × 70 μm² scan (b) 12 × 12 μm² and a selected cross-sectional scans (c) 2 × 2 μm² scan indicating porous structure of corrosion products.

197 Corrosion-induced changes of the second type
 198 have a localized character. They are seen even after
 199 exposure to HNO₃ vapors as short as 1 min and a
 200 subsequent storing in air for 24 h (Fig. 4). Most of
 201 the surface remained unchanged, however, a few
 202 protrusions indicating corrosion appeared. The
 203 protrusions grew in the form of regular structures
 204 of the overall diameter 2–12 μm, with a high cen-
 205 tral part surrounded by numerous lower circular
 206 structures. Fig. 4(b) shows the typical shape of the
 207 corrosion product. The central part is a uniform
 208 structure of the height of about 250 nm, whereas
 209 its surrounding is formed by granules with the siz-
 210 es diminishing when going further from the cen-
 211 ter. The porous surface of some protrusions (Fig.
 212 4(c)) suggests the location of the corrosion gas
 213 exits (NO₂, water vapor). It is worth to note that
 214 the height of the protrusions considerably exceeds
 215 the Fe(001) film thickness (50 nm) which means
 216 that the reaction products extend into the film bulk
 217 and that they have a porous structure of a dis-
 218 persed oxide/hydroxide.

219 The regular form of the corrosion products
 220 suggests that the corrosion proceeded on the sites
 221 of acid vapor condensation. The protrusions are
 222 distinctively higher in the central part than at the
 223 edge, obviously due to longer exposure to the ag-
 224 gressive solution in the center of the condensate
 225 droplet. The central part of the protrusion might

226 be also formed by the coalescence of smaller
 227 granules. Many of the corrosion centers reveal a
 228 hexagonal shape, which was reported previously
 229 by Oelkrug et al. [6].

230 Exposure of iron to HCl vapors resulted in
 231 similar effects as in the case of HNO₃. Addition-
 232 ally, we noticed enhanced localized corrosion
 233 along scratches of a mechanical origin (Fig. 5).
 234 Scratches can be more reactive than the intact
 235 surface for several reasons: (a) a bare metal, free of
 236 oxides could be exposed at scratches; (b) geomet-
 237 rical irregularities of the surface might be preferred
 238 condensation centers of vapors, and (c) kinks and
 239 steps on scratches are probably the most active
 240 reaction sites.

241 Corrosion products were identified by CEMS.
 242 Fig. 6(a) and (b) show CEMS spectra of 50 nm
 243 Fe(001) film after 25 h exposure to HNO₃ (com-
 244 pare Fig. 3(a)) and after 72 h exposure, respec-
 245 tively. The only noticeable change of the spectra,
 246 in comparison with the as-prepared sample (Fig.
 247 1(b)) is a doublet in the central part. The hyperfine
 248 parameters of the doublet, the isomer shift
 249 IS = 0.35 mm/s relative to metallic iron and
 250 quadrupole splitting QS = 0.74 mm/s indicate for
 251 a Fe³⁺ origin of the doublet, and are typical for
 252 different corrosion products observed on Fe sur-
 253 faces [13]. In a low temperature spectrum (85 K)
 254 the doublet remained magnetically unsplit, which

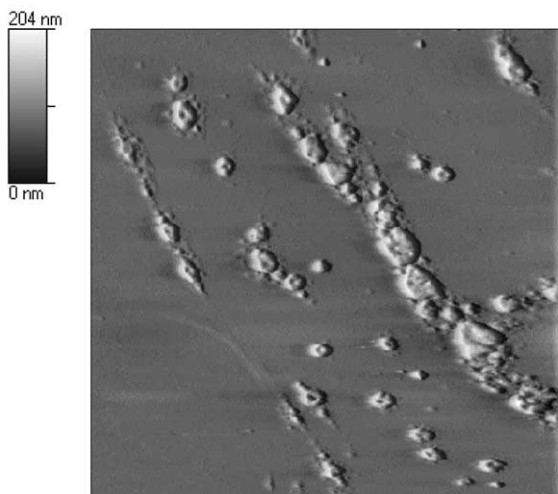


Fig. 5. AFM image ($25 \times 25 \mu\text{m}^2$) of an epitaxial Fe(001) film on MgO(001) after 1 min exposure to 1 M HCl vapors and subsequent 27 h storing in air. Corrosion products were formed on defects (scratches).

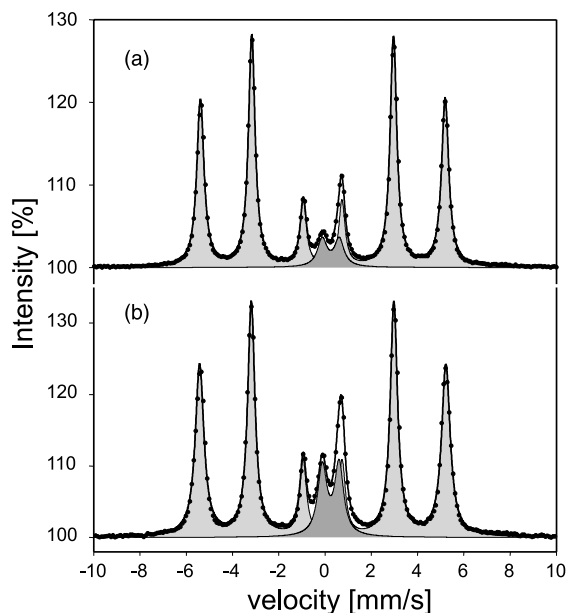


Fig. 6. CEMS spectra of a 50 nm epitaxial Fe(001) film on MgO(001) after exposure to 1 M HNO₃ vapors: (a) 25 h and (b) 72 h.

255 means that the corrosion product is most probably
256 γ -FeOOH. Prolongation of the exposure time

from 25 to 72 h increases the thickness of an
257 oxyhydroxide layer from 3.8 to 7.4 nm, as esti-
258 mated from the intensity of the spectral compo-
259 nents.
260

261 Exposure of the Fe/Fe₃O₄ film to HNO₃ vapors
262 resulted in much less pronounced changes of the
263 surface morphology and composition than it was
264 observed for a clean Fe(001) film. A post-expo-
265 sure STM topography revealed only a homoge-
266 neous increase of the surface roughness as
267 compared to in situ observation of the freshly
268 prepared surface. Similarly, no signs of chemical
269 surface modifications in the CEMS spectrum were
270 found after 15 min exposure. Further studies of the
271 Fe(001) surfaces passivated with the epitaxial
272 Fe₃O₄ layer are in progress.

273 The same corrosion product, γ -FeOOH, was
274 found by CEMS on the iron sample treated with
275 HCl vapors. However, the average depth of the
276 oxyhydroxide layer formed after 6 min exposure to
277 HCl vapors was two times larger than that after
278 72 h exposure to HNO₃.

5. Conclusions 279

280 Epitaxial Fe(001) films exposed to ambient at-
281 mosphere are highly resistant to corrosion. No
282 oxide layer thicker than 0.5 nm was found after a
283 one week exposure, which means that natural
284 passivation is very slow. Short exposure (minutes)
285 to HNO₃ and HCl vapors resulted in the appear-
286 ance of localized corrosion centers which cannot
287 be associated with any structural details and are
288 explained as coming from condensation of vapors.
289 Longer exposure (hours) results in the formation
290 of a homogeneous layer that was interpreted as γ -
291 FeOOH basing on CEMS measurements. The
292 corrosion process was studied previously on
293 polycrystalline iron films [10]. The oxide mor-
294 phology was highly diversified and the nucleation
295 of the corrosion products occurred at active sites
296 like steps, grain boundaries etc. On the surfaces of
297 the epitaxial films the localized corrosion is con-
298 nected probably with point defects (also mechan-
299 ical). Controlled oxidation of a surface iron layer
300 to epitaxial Fe₃O₄ passivates the film.

301 **Acknowledgements**

302 This work was partially supported by the Polish
 303 State Committee for Scientific Research, grant no.
 304 7 T08A 002 20.

305 **References**

- 306 [1] H.W. Pickering, T. Sakurai, NACE Conference “Corro-
 307 sion ’91”, Cincinnati, OH, 11–15 March, 1991, paper no.
 308 81.
 309 [2] P. Marcus, V. Maurice, in: K.E. Heusler (Ed.), Passivation
 310 of Metals and Semiconductors, Trans Tech, Switzerland,
 311 1994, p. 221.
 312 [3] P. Marcus, *Electrochim. Acta* 43 (1998) 109.
 313 [4] W.J. Lorenz, W. Plieth (Eds.), *Electrochemical Nanotech-*
 314 *nology. In situ Local Probe Techniques at Electrochemical*
 315 *Interfaces*, Wiley-VCH, Weinheim, 1998.

- [5] J. Karunamuni, R.L. Kurtz, R.L. Stockbauer, *Surf. Sci.* 316
 442 (1999) 223. 317
 [6] D. Oelkrug, M. Fritz, H. Stauch, *J. Electrochem. Soc.* 139 318
 (1992) 2419. 319
 [7] B. Müller-Züllow, S. Kipp, R. Lacmann, M.A. Schne- 320
 weiss, *Surf. Sci.* 311 (1994) 153. 321
 [8] O. Khaselev, J.M. Sykes, *Electrochim. Acta* 42 (1997) 322
 2333. 323
 [9] J. Li, D.J. Meier, *J. Electroanal. Chem.* 454 (1998) 53. 324
 [10] I. Flis-Kabulska, *J. Electroanal. Chem.* 508 (2001) 89. 325
 [11] J. Korecki, M. Kubik, N. Spiridis, T. Ślęzak, *Acta Physica* 326
Polonica A 97 (2000) 129. 327
 [12] S.M. Jordan, J.F. Lawler, R. Schad, H. van Kempen, J. 328
Appl. Phys. 84 (1998) 1499. 329
 [13] K. Nomura, Y. Ujihira, A. Vertes, *J. Radioanal. Nucl.* 330
Chem., Articles 202 (1996) 103. 331
 [14] J. Korecki, N. Spiridis, B. Handke, J. Prokop, J. Haber, 332
Electron Technol. 29 (1996) 269. 333
 [15] M.F. Toney, *Phys. Rev. Lett.* 79 (1997) 4282. 334
 [16] B. Stanka, W. Hebenstreit, U. Diebold, S.A. Chambers, 335
Surf. Sci. 448 (2000) 49. 336